Journal of Nuclear Materials 417 (2011) 77–80

Contents lists available at ScienceDirect

Journal of Nuclear Materials

journal homepage: www.elsevier.com/locate/jnucmat

Tensile and creep properties of reduced activation ferritic–martensitic steel for fusion energy application

M.D. Mathew [a,*], J. Vanaja [a], K. Laha [a], G. Varaprasad Reddy [a], K.S. Chandravathi [a], K. Bhanu Sankara Rao [b]

[a] Indira Gandhi Centre for Atomic Research, Kalpakkam 603 102, India
[b] Central University, Hyderabad, India

ARTICLE INFO

Article history:
Available online 1 February 2011

ABSTRACT

Tensile and creep properties of a reduced activation ferritic–martensitic (RAFM) steel for Indian Test Blanket Module (TBM) to be tested in ITER have been evaluated. The tensile strength was found to decrease with temperature; the rate of decrease being slower in the intermediate temperature range of 450–650 K. Tensile ductility of the steel decreased with increase in temperature up to 650 K, followed by a rapid increase beyond 650 K. Creep studies have been carried out at 773, 823 and 873 K over a stress range of 100–300 MPa. The variation of minimum creep rate with applied stress followed a power law, $\dot{\varepsilon}_m = A\sigma^n$. The '$n$' value decreased with increase in temperature. The creep rupture life was found to relate inversely with minimum creep rate through the Monkman–Grant relation, $t_r \cdot \dot{\varepsilon}_m$ = constant. The tensile and creep properties of the steel were comparable with those of Eurofer 97.

1. Introduction

Reduced activation ferritic–artensitic (RAFM) steels having 9–12% Cr are presently considered as main candidate materials for the TBM because of their inherent void swelling resistance coupled with low thermal expansion coefficient and high thermal conductivity compared to austenitic steels [1–3]. The requirement of safe operation and decommissioning of a fusion plant and disposal of radioactive wastes has also demanded the development of steels with reduced radioactive characteristics [4,5]. The process of developing India-specific RAFM steel containing W, Ta and V without Mo, Nb, Ni and other radiologically undesirable and embrittling elements is underway. As a late entrant to the fusion programme, India's strategy of development of the RAFM steel is as follows. In the first phase of the development, attempt has been made to develop a RAFM steel with composition conforming to Eurofer 97 to establish the capability of the Indian steel industry, for producing the steel with the specified chemistry and physical and mechanical properties. More alloys with different contents of W and Ta have been produced in the second phase of the development. Characterization of the physical and mechanical properties of these alloys is in progress. Based on the results of these studies, an India-specific RAFM steel will be specified. In the third phase of the development, detailed characterization of physical and mechanical properties of the India-specific steel will be carried out. This paper deals with the tensile and creep properties of the indigenously produced RAFM steel with specifications conforming to Eurofer 97.

2. Experimental

The RAFM steel was produced by M/s. Mishra Dhatu Nigam Limited (MIDHANI), Hyderabad, India. The measured chemical composition of the steel produced is shown in Table 1. The RAFM steel weighing around 200 kg has been produced by proper selection of pure raw materials, employing vacuum induction melting and vacuum arc remelting routes, and by exercising strict control over the thermomechanical processing parameters such as forging, rolling and heat treatments. The steel was subjected to the final heat treatment consisting of normalizing at 1250 K for 30 min followed by tempering at 1033 K for 60 min. Tensile tests were carried out in air over a temperature range of 300–923 K at a nominal stain rate of $3 \times 10^{-4}\,s^{-1}$. Strain rate was calculated from crosshead speed of the tensile machine with the assumption that only specimen in the load train deformed. Constant load creep tests were carried out at 773 K, 823 K and 873 K in air over a stress range of 100–300 MPa. Cylindrical tensile and creep specimens of 4 mm diameter, 20 mm gauge length and 5 mm diameter, 50 mm gauge length respectively were used. The temperature was maintained within ±2 K during the test and the creep elongation was monitored continuously by an extensometer with digimatic dial indicator and a data logger system.

3. Results and discussion

3.1. Microstructure

The as-received normalized and tempered RAFM steel has a tempered martensitic structure (Fig. 1). The lath like martensitic

* Corresponding author. Tel.: +91 44 2748 01017; fax: +91 44 2748 0075.
E-mail address: mathew@igcar.gov.in (M.D. Mathew).

0022-3115/$ - see front matter © 2011 Elsevier B.V. All rights reserved.
doi:10.1016/j.jnucmat.2011.01.058

Table 1
Chemical composition (wt.%) of the melted RAFM steel, compared with the specification of Eurofer 97.

Element	Cr	C	Mn	V	W	Ta	N	O	P	S
Melted RAFM steel	9.04	0.08	0.55	0.22	1.00	0.06	0.0226	0.0057	0.002	0.002
Eurofer 97	8.05–9.5	0.09–0.12	0.20–0.60	0.15–0.25	1.00–1.20	0.05–0.09	0.015–0.045	0.01 max	0.005 max	0.005 max
Element	B	Ti	Nb	Mo	Ni	Cu	Al	Si	Co	As + Sn + Sb + Zr
Melted RAFM steel	0.0005	<0.005	0.001	0.001	0.005	0.001	0.004	0.09	0.004	<0.03
Eurofer 97	0.001 max	0.01 max	0.001 max	0.005 max	0.005 max	0.005 max	0.01 max	0.05 max	0.005 max	0.05 max

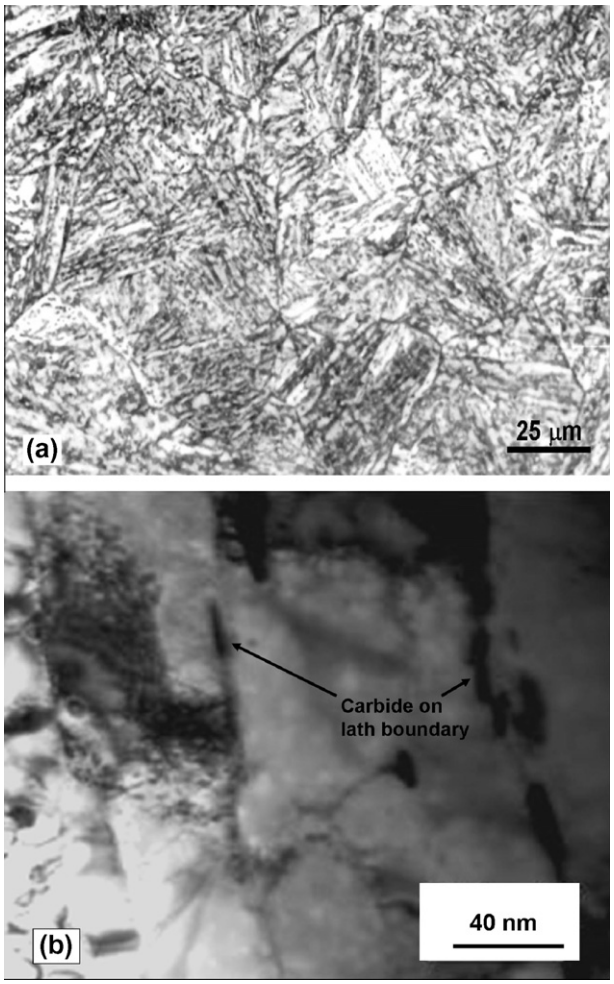

Fig. 1. Optical (a) and TEM (b) microstructures of the RAFM steel.

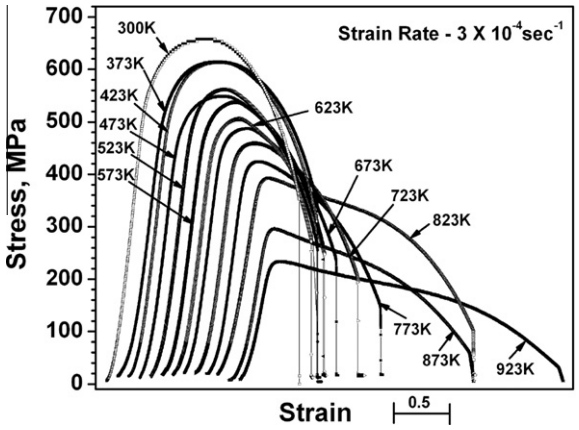

Fig. 2. Tensile stress–strain curves of the steel at different test temperatures.

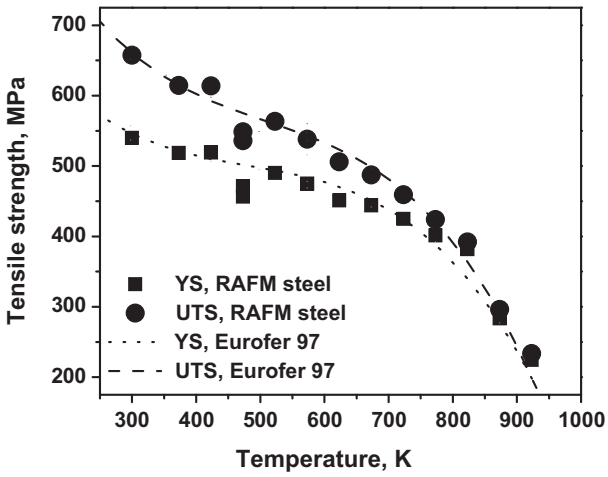

Fig. 3. Variation of yield strength and ultimate tensile strength of the steel with test temperature, compared with those of Eurofer 97 [9,10].

structure formed on normalization was found to retain even after the tempering treatment. The prior austenitic grain boundaries as well as the lath boundaries are decorated with carbides (Fig. 1b). The carbides are reported as of type $M_{23}C_6$ [6]. The steel derives its strength from the solid solution strengthening by tungsten, precipitate strengthening from intra- and inter-granular MX type ((V, Ta)C) carbides and transformation induced dislocation substructure [6].

3.2. Tensile properties

At a nominal strain rate of $3 \times 10^{-4}\,s^{-1}$, the steel exhibited monotonic smooth stress–strain curves over the entire temperature range employed (Fig. 2). No serrated flow was observed in the stress–strain curves. The variation in 0.2% offset yield strength (YS) and the ultimate tensile strength (UTS) with temperature are shown in Fig. 3 and compared with those of Eurofer 97. The yield strength and ultimate tensile strength of the steel are found to decrease with temperature having slower rate of decrease in the intermediate temperature range of 450–650 K. The slower rate of decrease in strength in the intermediate temperature range or even lower strength at lower temperature is attributed to dynamic strain ageing (DSA), even though no serration was observed in the stress–strain curves [7]. Serration is only one of the several manifestations of DSA [8]. The variation in total elongation and uniform elongation of the developed material is shown in Fig. 4 and compared with those of Eurofer 97. The total elongation of the steel decreased with increase in temperature up to 650 K, followed by a rapid increase beyond 650 K; similar trend was observed also for the variation of uniform elongation with temperature. The developed RAFM steel possesses tensile strength and ductility comparable to those of Eurofer 97 [9,10].

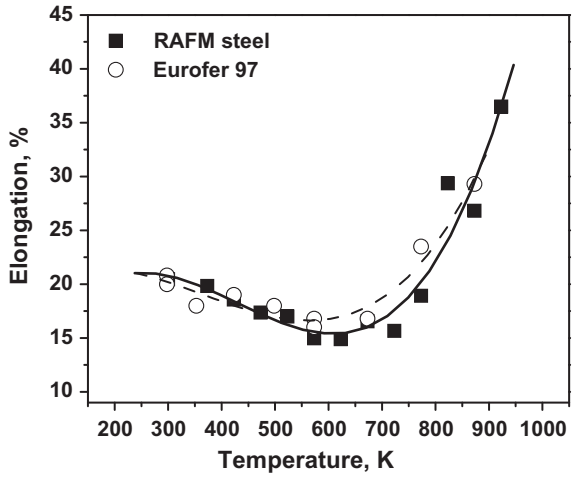

Fig. 4. Variation of total tensile elongation of the steel with test temperature, compared with that of Eurofer 97 [9,10].

3.3. Creep properties

The variations of creep strain with time at 823 K over the experimental applied stress range are shown in Fig. 5. The creep deformation is characterized by a very small strain on loading, a relatively brief primary stage followed by a prolonged tertiary stage. The material attained a minimum creep rate ($\dot{\varepsilon}_m$) before increase in the tertiary stage of deformation. The occurrence of minimum creep rate appears to result from a balance between hardening and recovery processes which are dominant in the primary and tertiary stages of creep deformation respectively. The variation of minimum creep rate ($\dot{\varepsilon}_m$) with applied stress (σ) is shown in Fig. 6. The minimum creep rate increased with increase in stress and temperature. The $\dot{\varepsilon}_m$ vs. σ variation obeyed a power law relation of the form $\dot{\varepsilon}_m = A\sigma^n$, where A is a constant. The stress exponent 'n' was found to decrease with increase in temperature. A plot of normalized creep rate ($\dot{\varepsilon}_m KT/DGb$) vs. normalized ($\sigma/G$), where k is Boltzmann's constant, T is the absolute temperature, D is the diffusion coefficient, G is the shear modulus, and b is the Burgers vector, is shown in Fig. 7. The creep rate data at different test temperatures could be represented by a single line with stress exponent 'n' of 10.05. The observed values of 'n' are high compared to a value of 4–5, as predicted by diffusion controlled models of dislocation creep. High value of 'n' and its decrease with temperature have been reported by several investigators in ferritic steels including RAFM steels and is attributed to the coarsening of MX carbides which reduces the coherent strain between precipitate and matrix [11,12]. The variation of rupture life (t_r) of the material with applied stress at different temperatures is shown in Fig. 8.

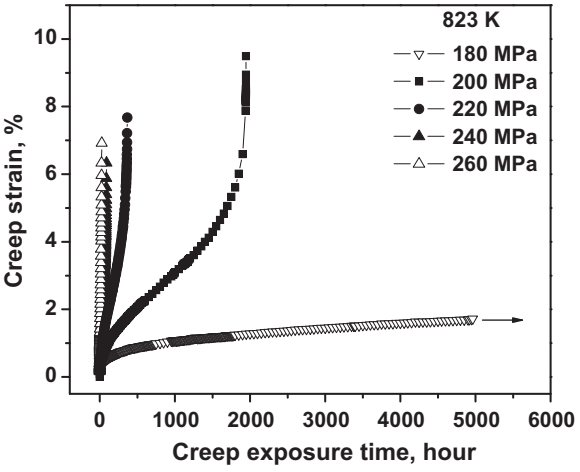

Fig. 5. Creep curves of the steel at 823 K over the applied stress range of 180–260 MPa.

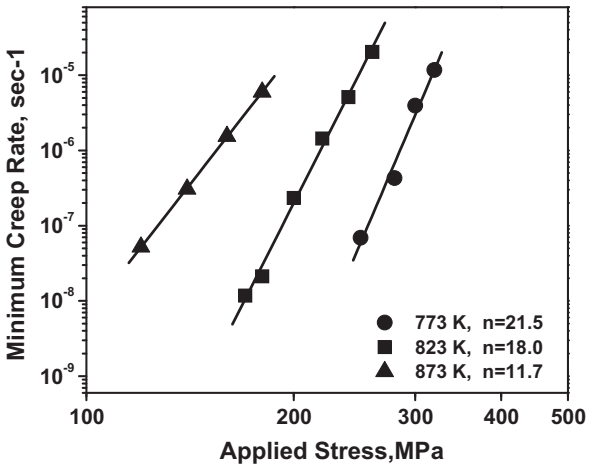

Fig. 6. Variation of minimum creep rate of the steel with applied stress.

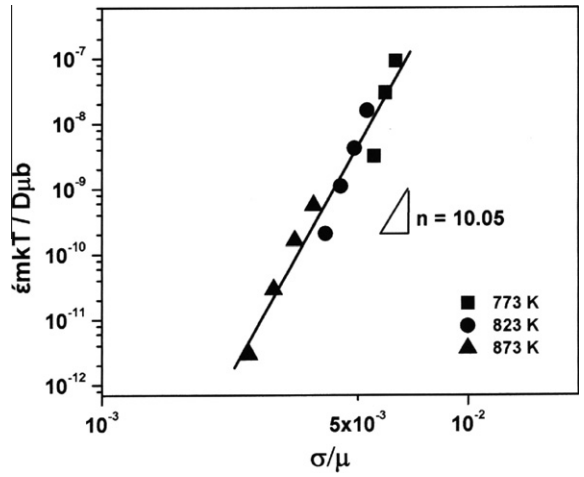

Fig. 7. Variation of temperature compensated minimum creep rate with normalized stress of the steel.

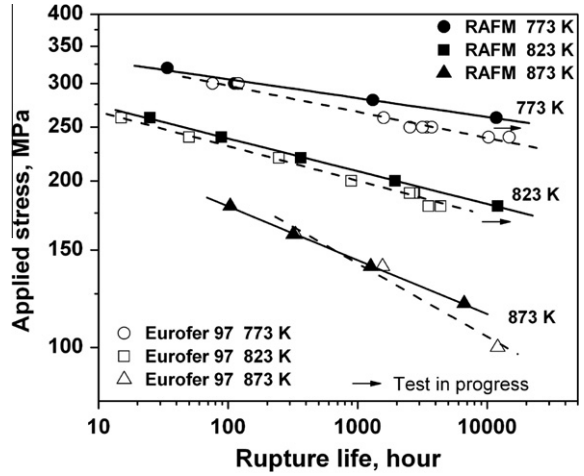

Fig. 8. Variation of rupture life with applied stress of the steel, compared with that of Eurofer 97 [9,10].

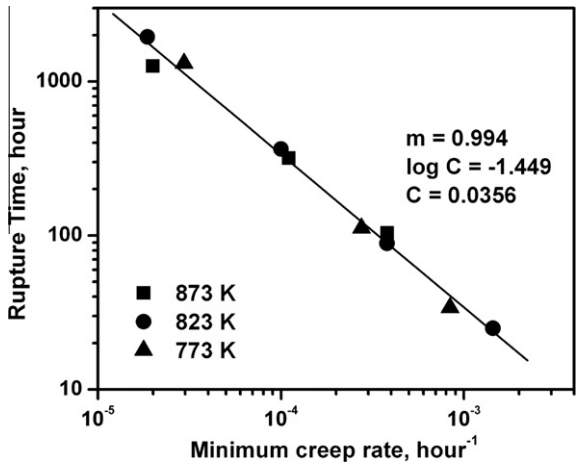

Fig. 9. Variation of rupture life with minimum creep rate of the steel (Monkman–Grant relation).

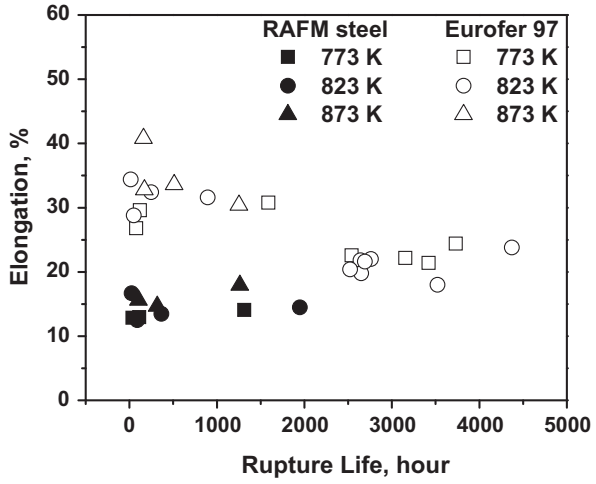

Fig. 10. Variation of rupture elongation with rupture life of the steel, as compared with Eurofer 97 [9,10].

Creep rupture strength of the material is comparable to that of Eurofer 97 [9,10]. The stress dependence of rupture life also obeyed a power law relation, $t_r = A'\sigma^{-n'}$. The variation of minimum creep rate with rupture life is shown in Fig. 9. The variation obeys the Monkman–Grant relation $\dot{\varepsilon}_{min} \cdot t_r$ = constant, signifying that same mechanism was responsible for creep deformation and fracture. The variation of percentage elongation as a function of rupture life is shown in Fig. 10 and compared to those of Eurofer 97. The developed RAFM steel has rupture ductility lower to that of Eurofer 97 [9,10]. The steel had prior austenitic grain size of ≈15 μm against 6.7–11 μm reported for Eurofer 97 due to the lower content of tantalum 0.06 wt.% against 0.14 wt.% in Eurofer 97 (heat – 83698) [6]. Larger grain size of the steel might be a reason for the slightly lower creep ductility than Eurofer 97.

4. Conclusions

Creep deformation of RAFM steel is characterized by relatively short primary stage with prolonged tertiary creep regime. The stress dependence of minimum creep rate obeyed power law relation with high value of stress exponent that increased with decrease in temperature. The minimum creep rate and rupture life of the steel followed the Monkman–Grant relation. The developed steel possessed tensile and creep rupture strength and ductility comparable to the internationally developed Eurofer 97 RAFM steel.

Acknowledgements

The authors thank Dr. Baldev Raj, Director, Indira Gandhi Centre for Atomic Research and Dr. T. Jayakumar, Director, Metallurgy and Materials Group for their keen interest in this work.

References

[1] Akira Kohyama, Yutaka Kohno, J. Nucl. Mater. 212–215 (1994) 684–689.
[2] N. Baluc, R. Schaublin, P. Spatig, M. Victoria, Nucl. Fission 44 (2004) 56–61.
[3] G.L. Butterworth, J. Nucl. Mater. 179–181 (1991) 135.
[4] I. Cook, D. Ward, S. Dudarev, Plasma Phys. Controlled Fusion 44 (2002) B121–B136.
[5] R. Lindau et al., Fusion Eng. Des. 75–79 (2005) 989–996.
[6] P. Fernández, A.M. Lancha, J. Lapeña, M. Harnández-Mayoral, Fusion Eng. Des. 58–59 (2001) 787–792.
[7] Hualin Li, A. Nishimura, T. Nagasaka, T. Muroga, Fusion Eng. Des. 81 (2006) 2907–2912.
[8] P. Rodriguez, Bull. Mater. Sci. 6 (1984) 635.
[9] M. Reith, M. Schirra, A. Falkenstein, P. Grof, S. Heger, H. Kempe, R. Lindau, H. Zimmermann, EUROFER 97 Tensile, Charpy, Creep and Structural Tests, Forschungszentrum Karlsruhe, Germany, KZKA 6911 Report, 2003.
[10] A.F. Tavassoli et al., J. Nucl. Mater. 329–333 (2004) 257–262.
[11] P. Fernández, A.M. Lancha, J. Lapeña, R. Lindau, M. Rieth, M. Schirra, Fusion Eng. Des. 75–79 (2005) 1003–1008.
[12] K. Sawada, K. Kubo, F. Abe, Mater. Sci. Eng. A319–A321 (2001) 784–787.